

Efficacy of Camptothecin Analog DX-8951f (Exatecan Mesylate) on Human Pancreatic Cancer in an Orthotopic Metastatic Model¹

Fang-Xian Sun, Akiko Tohgo, Michael Bouvet, Shigeo Yagi, Rounak Nassirpour, Abdoul R. Moossa, and Robert M. Hoffman²

AntiCancer, Inc., San Diego, California 92111 [F.-X. S., S. Y., R. M. H.]; Daiichi Pharmaceutical Co., Ltd., Tokyo 134-8630, Japan [A. T.]; and Department of Surgery, University of California, San Diego, San Diego, California 92161 [M. B., R. N., A. R. M., R. M. H.]

ABSTRACT

We determined the antitumor and antimetastatic efficacy of the camptothecin analogue DX-8951f in an orthotopic metastatic mouse model of pancreatic cancer. DX-8951f showed efficacy against two human pancreatic tumor cell lines in this model. These cell lines were transduced with the green fluorescent protein, enabling high-resolution visualization of tumor and metastatic growth *in vivo*. The DX-8951f studies included both an early and advanced cancer model. In the early model, using the human pancreatic cancer lines MIA-PaCa-2 and BxPC-3, treatment began when the orthotopic primary tumor was ~7 mm in diameter. DX-8951f was significantly effective against both MIA-PaCa-2 and BxPC-3. In contrast, 2', 2'-difluorodeoxycytidine (gemcitabine), the standard treatment for pancreatic cancer, did not have significant efficacy against MIA-PaCa-2. Although gemcitabine showed significant activity against BxPC-3 primary tumor growth, it was not effective on metastasis. In the model of advanced disease, using BxPC-3, treatment started when the orthotopic primary tumor was 13 mm in diameter. DX-8951f was significantly effective in a dose-response manner on the BxPC-3 primary tumor. DX-8951f also demonstrated antimetastatic activity in the late-stage model, significantly reducing the incidence of lymph node metastasis while eliminating lung metastasis. In contrast, gemcitabine was only moderately effective against the primary tumor and ineffective against metastasis at both sites in the late-stage model. Therefore, DX-8951f was highly effective against primary and metastatic growth in this very difficult-to-treat disease and showed significantly higher efficacy than gemcitabine, the standard treatment of pancreatic cancer. DX-8951f, therefore, has important clinical promise and has more positive features than the currently used camptothecin analogue CPT-11, which requires metabolic activation and is toxic.

INTRODUCTION

Effective new drugs are urgently needed for pancreatic cancer. Pancreatic cancer is the fifth leading cause of cancer death in the United States (1). This year ~28,000 Americans will die from cancer of the pancreas. The average life expectancy after being diagnosed with pancreatic cancer is 3–6 months. Reasons for low survival in this disease include aggressive tumor biology, high metastatic potential, and late presentation at the time of diagnosis (2). The chemotherapeutic agent most commonly used to treat metastatic cancer of the pancreas is gemcitabine³ (3). This nucleoside analogue inhibits cellular repair, induces apoptosis, and is a potent radiosensitizer of rodent and human tumor cells.

Camptothecin (CPT) is an alkaloid extracted from *Camptotheca acuminata*. CPT binds to topoisomerase I, an enzyme that relaxes the supercoiled DNA duplex during replication and transcription (4). Be-

cause tumor cells have been shown to contain more topoisomerase I compared with normal tissue, CPT and its analogs are good candidates for specific cancer treatment. Irinotecan (CPT-11) and topotecan are the most widely used CPT analogues in clinical use and in trials against colon cancer (4). These CPTs contain a terminal lactone ring that makes them unstable in aqueous solutions by undergoing a rapid, pH-dependent, nonenzymatic hydrolysis to form an open-ring hydroxy carboxylic acid. This hydrolysis makes them much less potent inhibitors of topoisomerase I.

Recent trials have added irinotecan to gemcitabine in an attempt to increase efficacy (5). The irinotecan/gemcitabine combination offers encouraging activity in terms of radiographic and tumor marker CA 19-9 response and increased 1-year survival in pancreatic cancer (27%). This regimen is well tolerated, with minimal grade-3 and

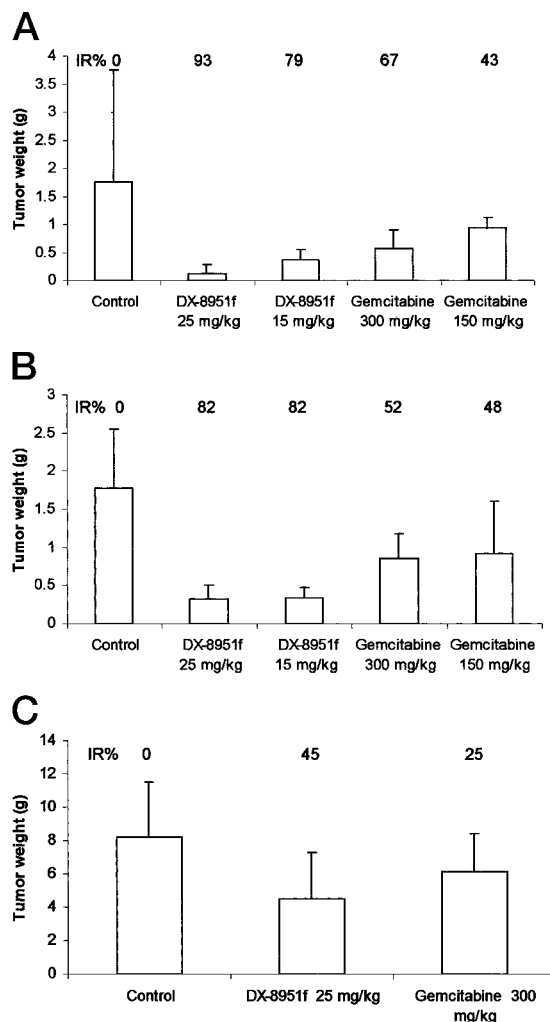


Fig. 1. The mean final primary tumor weight for MIA-PaCa-2 (A) and BxPC-3 (B) early-stage orthotopic human pancreatic models treated with 15 and 25 mg/kg DX-8951f and 150 and 300 mg/kg gemcitabine compared with the control. C, BxPC-3 late-stage model treated with 25 mg/kg DX-8951f and 300 mg/kg gemcitabine compared with control.

Received 8/7/02; accepted 10/31/02.

The costs of publication of this article were defrayed in part by the payment of page charges. This article must therefore be hereby marked *advertisement* in accordance with 18 U.S.C. Section 1734 solely to indicate this fact.

¹ This study was supported in part by the National Cancer Institute grant 1R43 CA89779-01.

² To whom requests for reprints should be addressed, at AntiCancer, Inc., 7917 Ostrow Street, San Diego, CA 92111. Phone: (858) 654-2555; Fax: (858) 268-4175; E-mail: all@anticancer.com.

³ The abbreviations used are: gemcitabine, 2', 2'-difluorodeoxycytidine; CPT, camptothecin; SOI, surgical orthotopic implantation; GFP, green fluorescent protein; IR, inhibition rate; IR%, percentage of inhibition rate.

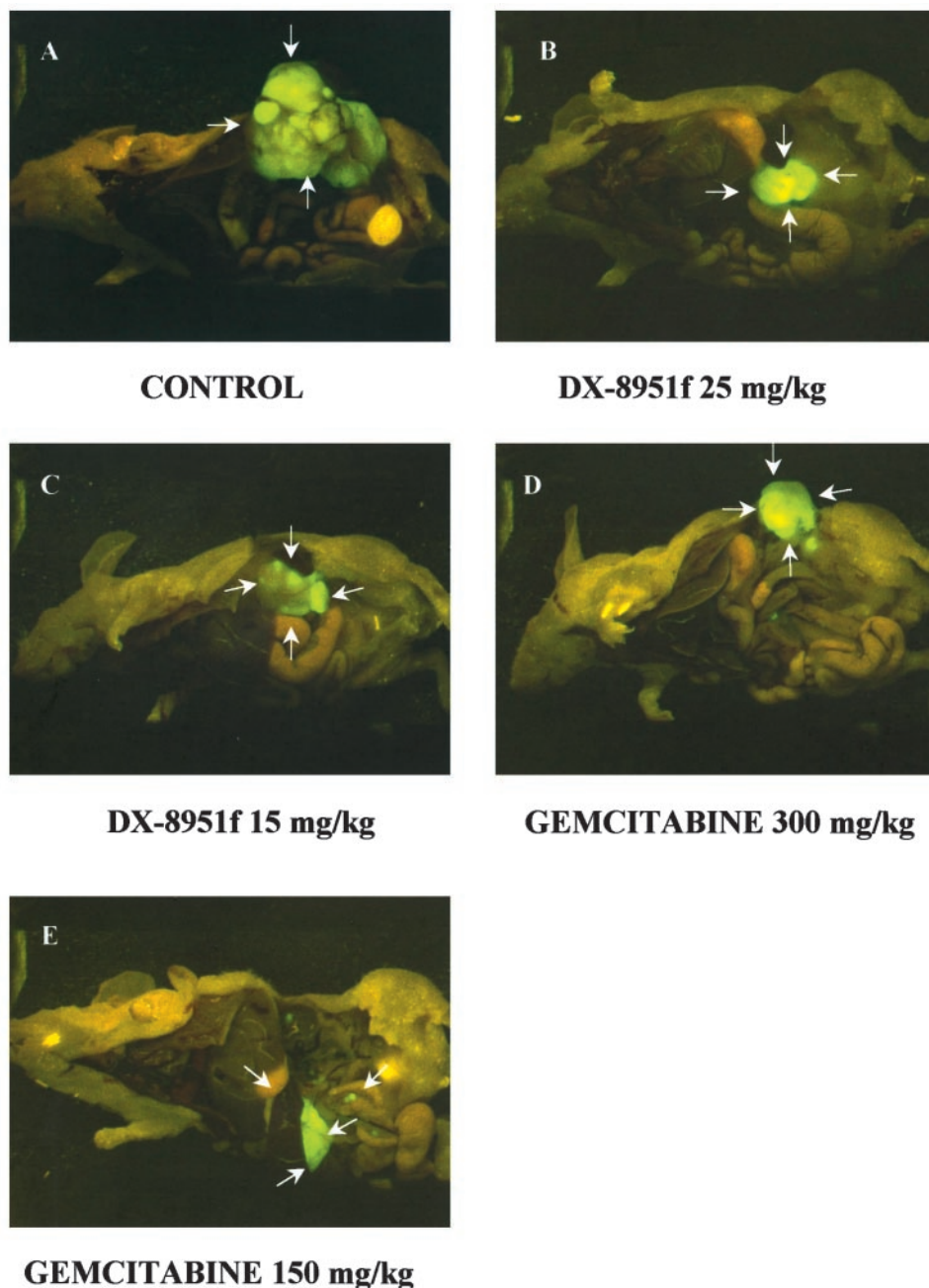


Fig. 2. GFP images of primary tumors in the MIA-PaCa-2 early-stage model shown for each treatment group on day 42 of the study. *A*, control. *B*, 25 mg/kg DX-8951f. *C*, 15 mg/kg DX-8951f. *D*, 300 mg/kg of gemcitabine. *E*, 150 mg/kg gemcitabine. White arrows show the primary pancreatic tumor. See “Materials and Methods” for imaging procedure.

grade-4 toxicities and excellent maintenance of planned dose intensity. Despite these encouraging results, the median survival of these patients was still only 5.7 months, indicating additional need for improvement.

DX-8951f is a synthetic analogue of CPT with increased solubility and antitumor efficacy *in vitro* (6–10). Previous studies have shown DX-8951f to be active against human cancer cell lines *in vitro*, including pancreatic cancer (7–10). DX-8951f was also shown to be active in s.c. xenograft models, including pancreatic cancer (7, 11). However, these models are limited in that the tumors are growing in an ectopic microenvironment and do not metastasize. In this study, we examined the *in vivo* antitumor activity of DX-8951f against SOI models of human pancreatic tumors BxPC-3 and MIA-PaCa-2 (12, 13). In this model, the tumor grows in its natural tissue microenvironment enabling a clinical-like pattern of metastasis to ensue. In the present studies, comparison was made in the SOI models with DX-8951f and gemcitabine, the treatment standard for pancreatic cancer.

MATERIALS AND METHODS

Pancreatic Cancer Cell Lines

The BxPC-3 and MIA-PaCa-2 human pancreatic cancer cell lines were obtained from the American Type Culture Collection (Rockville, MD). The cells were maintained in DMEM supplemented with 10% FCS, 2 mM glutamine, 100 units/ml penicillin, 100 μ g/ml of streptomycin, and 0.25 μ g/ml of amphotericin B (Life Technologies, Inc., Grand Island, NY). Both cell lines were incubated at 37°C in 5% CO₂.

GFP-Retroviral Transduction and Selection of High GFP-Expression MIA-PaCa-2 and BxPC-3 Pancreatic Cancer Cells

The retroXpress vector pLEIN was purchased from Clontech Laboratories, Inc. (Palo Alto, CA). The pLEIN vector expresses enhanced GFP and the neomycin resistance gene on the same bicistronic message. pLEIN was produced in PT67 packaging cells. For GFP gene transduction, 20% confluent MIA-PaCa-2 or BxPC-3 cells were incubated with a 1:1 precipitated mixture of retroviral supernatants of the PT67 packaging cells and RPMI 1640 (Life

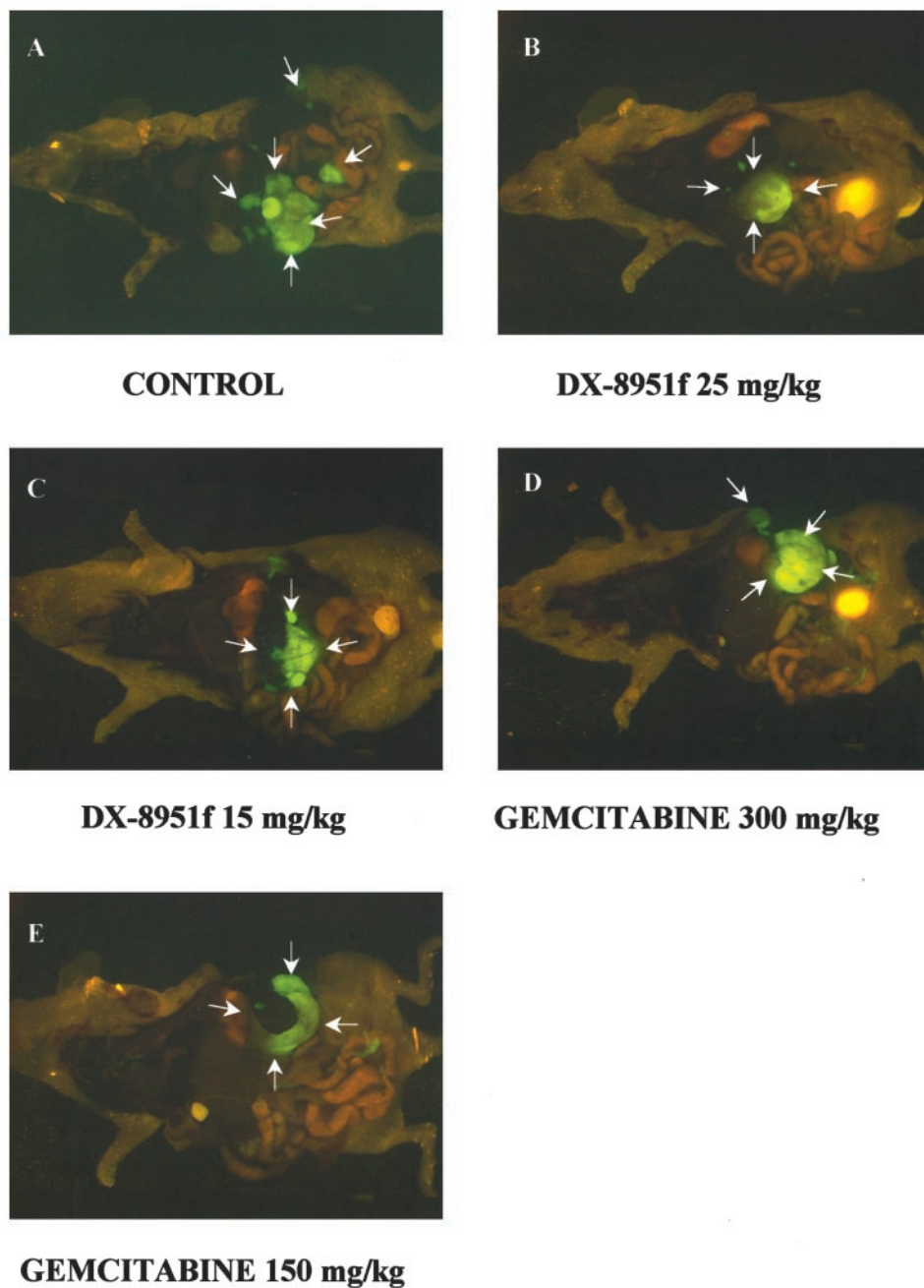


Fig. 3. GFP images of primary tumor and metastases of early-stage model of BxPC-3 taken on day 28 of the study. A, control. B, 25 mg/kg DX-8951f. C, 15 mg/kg DX-8951f. D, 300 mg/kg gemcitabine. E, 150 mg/kg gemcitabine. White arrows indicate the primary tumor and the peripheral metastases.

Technologies, Inc.) for 72 h. Fresh medium was replenished at this time. MIA-PaCa-2 or BxPC-3 cells were harvested by trypsin/EDTA 72 h after infection with the GFP retroviral supernatants. The cells were then subcultured at a ratio of 1:15 into selective medium that contained 200 $\mu\text{g/ml}$ of G418. The level of G418 was increased to 1000 $\mu\text{g/ml}$ stepwise. MIA-PaCa-2 and BxPC-3 clones expressing GFP (MIA-PaCa-2-GFP or BxPC-3-GFP) were isolated with cloning cylinders (Bel-Art Products, Pequannock, NJ) by trypsin/EDTA. The clones were amplified and transferred by conventional culture methods. High GFP-expression clones were then isolated in the absence of G418 for >10 passages to select for stable expression of GFP (14).

Animals

Female nude mice (NCr-nu) between 5 and 6 weeks of age were maintained in a barrier facility on HEPA-filtered racks. The animals were fed with autoclaved laboratory rodent diet (Teckland LM-485; Western Research Products, Orange, CA). All animal studies were conducted in accordance with the

principles and procedures outlined in the NIH Guide for the Care and Use of Animals under assurance number A3873-1.

SOI

Pancreatic tumors, grown s.c. in nude mice, were harvested at the exponential growth phase and resected under aseptic conditions. Necrotic tissues were cut away, and the remaining healthy tumor tissues were cut with scissors and minced into $\sim 1 \text{ mm}^3$ pieces in HBSS containing 100 units/ml penicillin and 100 $\mu\text{g/ml}$ streptomycin. For SOI, mice were anesthetized with isoflurane. The abdomen was sterilized with iodine, and an incision was made through the left upper abdominal pararectal line and peritoneum. The pancreas was carefully exposed and three tumor pieces were transplanted on the middle of the pancreas with an 8-0 Dexon (Davis-Geck, Inc., Manati, Puerto-Rico) surgical suture. The pancreas was then returned to the peritoneal cavity, the abdominal wall, and the skin were closed with 6-0 Dexon sutures. Animals were kept in a sterile environment. All procedures of the operation described above were

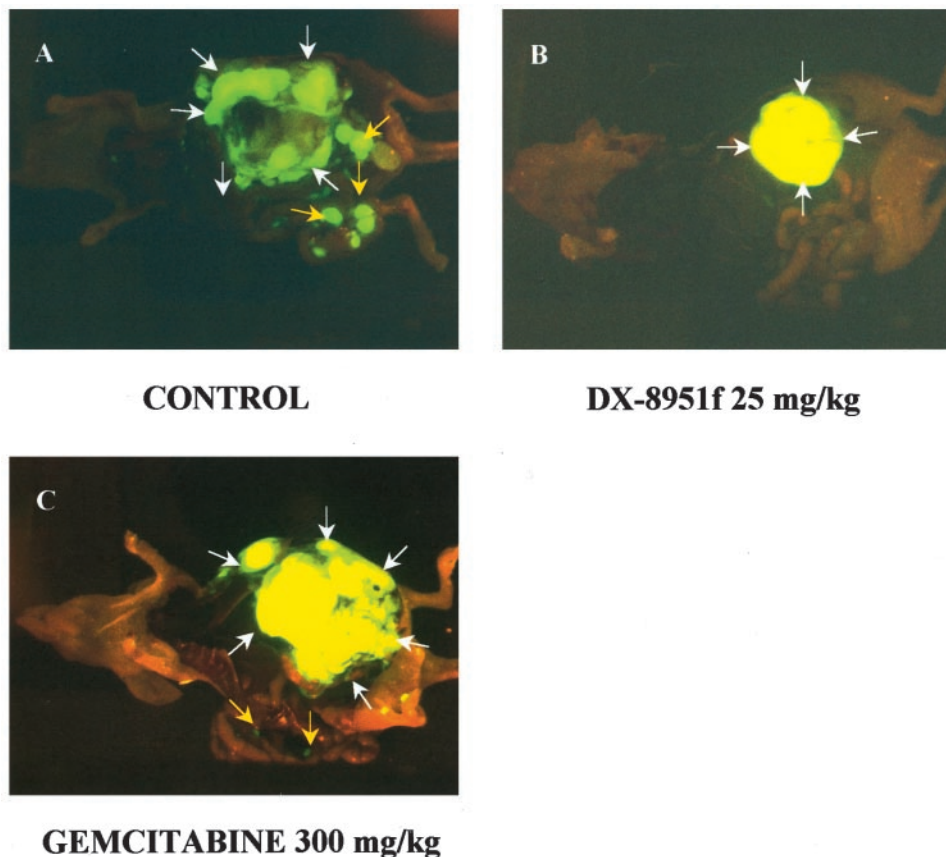


Fig. 4. GFP images of primary tumor and metastases of late-stage model of BxPC-3 on day 56. A, control. B, DX-8951f (25 mg/kg; no lymphatic metastases were found). C, gemcitabine (300 mg/kg). White arrows indicate primary tumor; yellow arrows indicate lymphatic metastases.

performed with a 7 \times microscope (Olympus) under HEPA-filtered laminar flow hoods (15).

In Vivo Drug Studies

DX-8951f (Daiichi Pharmaceutical Co., Ltd., Montvale, NJ) was diluted in water and administered i.v. Gemcitabine (Eli Lilly, Indianapolis, IN) was reconstituted in saline and administered i.p. Dosing for both drugs was performed once a week for 3 weeks.

Early Cancer Model. At 3 weeks after BxPC-3-GFP and MIA-PaCa-2-GFP orthotopic implantation, mice were randomized into five different groups of 5 mice each for treatment purposes. Group 1 served as the negative control and did not receive any treatment. Groups 2 and 3 were treated with DX-8951f at 25 and 15 mg/kg/dose, respectively. Groups 4 and 5 received gemcitabine treatments at 300 and 150 mg/kg/dose, respectively.

Late Cancer Model. At 6 weeks after BxPC-3-GFP orthotopic implantation, mice were randomized into three different groups of 20 mice each for treatment purposes. Group 1 served as the negative control and did not receive any treatment. Group 2 was treated with 25 mg/kg/dose DX-8951f and group 3 received 300 mg/kg/dose gemcitabine. Dosing for both drugs was performed once a week for 3 weeks, discontinued for 2 weeks, and then continued for another 3 weeks.

In both early and late cancer models, primary tumor size and body weights were measured once a week. Tumor volumes were calculated using the formula $a \times b^2 \times 0.5$, where a and b represent the larger and smaller diameters, respectively. At the termination of the studies, mice were sacrificed and explored. Final tumor weights and direct GFP images of primary tumor and metastases were recorded for each mouse (please see below). The tumor growth IR was calculated using the formula $IR (\%) = (1 - TWt/TWc) \times 100$, where TWt and TWc are the mean tumor weight of treated and control groups, respectively.

Microscopy

A Leica fluorescence stereo microscope model LZ12 (Leica Microsystems, Inc., Bannockburn, IL) equipped with a mercury 50-W lamp power supply was

used. Selective excitation of GFP was produced through a D425/60 band-pass filter and 470 DCXR dichroic mirror. Emitted fluorescence was collected through a long-pass filter GG475 (Chroma Technology, Brattleboro, VT) on a Hamamatsu C5810 3-chip cooled color CCD camera (Hamamatsu Photonics Systems, Bridgewater, NJ). Periodically, the tumor-bearing mice were also imaged in a fluorescence light box illuminated by fiberoptic lighting at 490 nm with images collected with the Hamamatsu camera described above (Lighttools Research, Inc., Encinitas, CA). High resolution images of 1024 \times 724 pixels were captured directly on an IBM PC or continuously through video output on a high resolution Sony VCR model SLV-R1000 (Sony Corp., Tokyo, Japan). Images were processed for contrast and brightness and analyzed with the use of Image Pro Plus 3.1 software (Media Cybernetics, Silver Spring, MD; Ref. 16).

Histological Analysis

Tissue samples of the primary tumor and lungs were processed for H&E staining for microscope examination. Lung metastasis was evaluated by histological examination under light microscopy.

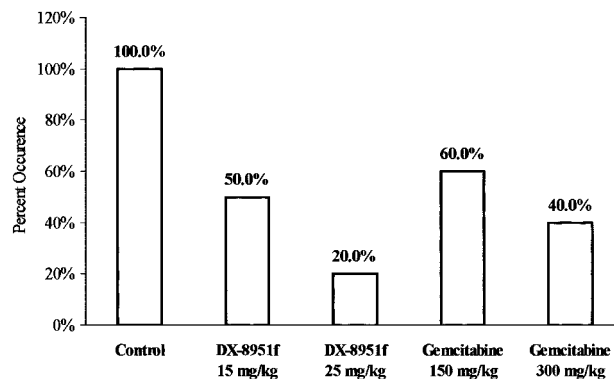


Fig. 5. Occurrence of lymphatic metastasis in DX-8951f- and gemcitabine-treated early-stage model of BxPC-3.

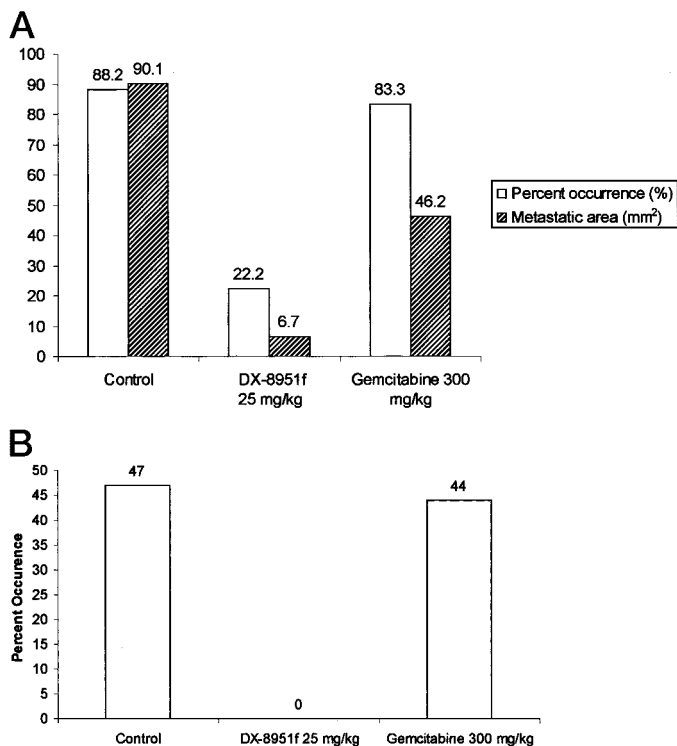


Fig. 6. Occurrence and total area of lymphatic metastasis (A) and occurrence of lung metastases (B) of late-stage model of BxPC-3 treated with DX-8951f or gemcitabine compared with control groups.

Statistical Analysis

The two-tailed *t* test was used to measure differences in final tumor weights, body weights, and total areas of metastatic foci among the various groups. The two-tailed Fisher's exact test was used to compare tumor metastatic rates between groups. The statistical analysis was performed on the data collected from animals that survived the duration of the study. A $P \leq 0.05$ was considered to be statistically significant.

RESULTS AND DISCUSSION

Early Cancer Model

MIA-PaCa-2-GFP. DX-8951f at doses of 25 and 15 mg/kg significantly inhibited MIA-PaCa primary tumor growth (Figs. 1A and 2). The mean final tumor weight showed significant differences in those animals treated at both doses of DX-8951f compared with the control ($P = 0.049$ for 15 mg/kg and $P = 0.020$ for 25 mg/kg). The tumor growth IR (IR%) was 93% for DX-8951f at 25 mg/kg and 79% for DX-8951f at 15 mg/kg compared with control (Figs. 1A and 2). Gemcitabine did not significantly inhibit MIA-PaCa-2 primary tumor growth. The tumor growth IR (IR%) of gemcitabine was 67%

($P = 0.105$) and 47% ($P = 0.233$) for the high and low dose, respectively (Figs. 1A and 2).

BxPC-3-GFP. DX-8951f at doses of 15 and 25 mg/kg significantly inhibited BxPC-3 primary tumor growth compared with control ($P = 0.001$, 0.000 respectively; Figs. 1B and 3). The IR% was 82% for DX-8951f at 25 mg/kg and 15 mg/kg (Figs. 1B and 3). DX-8951f inhibited BxPC-3 lymphatic metastasis formation in a dose-dependent manner in the early cancer model ($P = 0.048$; Figs. 4 and 5). Gemcitabine inhibited BxPC-3 primary tumor growth less than DX-8951f in the early cancer model with an IR of only 51.7% ($P = 0.017$) and 48% ($P = 0.025$) for the high and low dose, respectively (Figs. 1B, and 3). The dose-dependent inhibition of the occurrence of lymphatic metastases was greater for DX-8951f than gemcitabine (Fig. 5).

BxPC-3 Late-stage Cancer Model. DX-8951f was effective against BxPC-3 lymphatic metastasis and completely eliminated lung metastasis (Fig. 6). In contrast to DX-8951f, gemcitabine (300 mg/kg) had no effect on the occurrence of BxPC-3 (25 mg/kg) lymphatic or lung metastasis in the late-stage model (Fig. 6). DX-8951f (25 mg/kg) was more effective in inhibition of BxPC-3 primary tumors than gemcitabine (300 mg/kg). The IR of DX-8951f was 45 versus 25% for gemcitabine in the late-stage model (Fig. 1C).

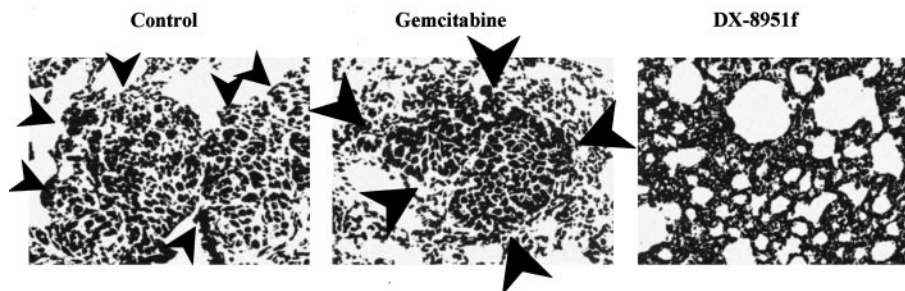
These results are also seen when the total GFP lymphatic metastasis were quantified using optical imaging at sacrifice (Fig. 6A). The results indicate that DX-8951f (25 mg/kg) significantly inhibited BxPC-3 lymphatic metastasis compared with control ($P = 0.000$). In contrast, gemcitabine (300 mg/kg) did not significantly inhibit lymphatic metastasis (Fig. 6A).

In addition, the occurrence of lung metastasis was examined by histological analysis under light microscopy on the day of sacrifice. The results indicated that DX-8951f (25 mg/kg) completely prevented BxPC-3 lung metastasis ($P = 0.001$), whereas gemcitabine had no effect on lung metastasis formation (Figs. 6B and 7) in the late-stage model.

Thus, DX-8951f is a more potent antitumor and antimetastatic drug in both early- and late-stage models compared with gemcitabine. In both pancreatic cancer models, DX-8951f inhibited tumor growth and had a higher tumor growth IR compared with gemcitabine. In the early cancer model, gemcitabine was ineffective in inhibition of the primary MIA-PaCa-2 tumor and did not inhibit metastasis of BxPC-3. In the late cancer model, DX-8951f inhibited lymphatic metastasis and eliminated lung metastasis of BxPC-3, whereas gemcitabine had no antimetastatic efficacy. Thus, DX-8951f is more effective than gemcitabine against primary human pancreatic tumor growth and metastasis in orthotopic nude mouse models thereby showing significant promise against a currently intractable disease. Promising clinical results in Phase I and Phase II trials have now been observed for DX-8951f (17, 18). With the results of this article, clinical trials can now be designed to evaluate DX-8951f in both early and advanced metastatic pancreatic cancer.

An important feature of the study was the use of the orthotopic

Fig. 7. H&E section of BxPC-3 lung metastases obtained from the control, gemcitabine (300 mg/kg)- and DX-8951f (25 mg/kg)-treated late-stage model. Gemcitabine was a poor inhibitor of metastases as shown here. In contrast, DX-8951f completely inhibited the occurrence of lung metastases. The black arrows indicate lung micro-metastases.



model that enabled the metastatic potential of the human pancreatic tumors to be expressed in nude mice. In particular, the SOI model has been demonstrated to be a clinically relevant orthotopic model (19). The use of GFP gave significant added power to the SOI model, enabling the observation of metastasis at the single cell level (20). The antimetastatic efficacy of DX-8951f in this SOI model, therefore, is all the more impressive, given that the model enabled high metastasis frequencies in the untreated animals that could be detected with the ultra high-resolution of GFP.

REFERENCES

- Jemal, A., Thomas, A., Murray, T., and Thun, M. Cancer statistics, 2002. *CA - Cancer J. Clin.*, *52*: 23–47, 2002.
- Bouvet, M., Binmoeller, K. F., and Moossa, A. R. Diagnosis of adenocarcinoma of the pancreas. In: J. L. Cameron (ed.), *American Cancer Society Atlas of Clinical Oncology: Pancreatic Cancer*. Hamilton, Ontario, Canada: BC Decker, 2001.
- Burris, H. A., III, Moore, M. J., Andersen, J., Green, M. R., Rothenberg, M. L., Modiano, M. R., Cripps, M. C., Portenoy, R. K., Storniolo, A. M., Tarassoff, P., Nelson, R., Dorr, F. A., Stephens, C. D., and Von Hoff, D. D. Improvements in survival and clinical benefit with gemcitabine as first-line therapy for patients with advanced pancreas cancer: a randomized trial. *J. Clin. Oncol.*, *15*: 2403–2413, 1997.
- Takimoto, C. H., Wright, J., and Arbut, S. G. Clinical applications of the camptothecins. *Biochim. Biophys. Acta*, *1400*: 107–119, 1998.
- Rocha Lima, C. M., Savarese, D., Bruckner, H., Dudek, A., Eckardt, J., Hainsworth, J., Yunus, F., Lester, E., Miller, W., Saville, W., Elfring, G. L., Locker, P. K., Compton, L. D., Miller, L. L., and Green, M. R. Irinotecan plus gemcitabine induces both radiographic and CA 19-9 tumor marker responses in patients with previously untreated advanced pancreatic cancer. *J. Clin. Oncol.*, *20*: 1182–1191, 2002.
- Mitsui, I., Kumazawa, E., Hirota, Y., Aonuma, M., Sugimori, M., Ohsuki, S., Uoto, K., Ejima, A., Terasawa, H., and Sato, K. A new water-soluble camptothecin derivative, DX-8951f, exhibits potent antitumor activity against human tumors *in vitro* and *in vivo*. *Jpn. J. Cancer Res.*, *86*: 776–782, 1995.
- Takiguchi, S., Kumazawa, E., Shimazoe, T., Tohgo, A., and Kono, A. Antitumor effect of DX-8951, a novel camptothecin analog, on human pancreatic tumor cells and their CPT-11-resistant variants cultured *in vitro* and xenografted into nude mice. *Jpn. J. Cancer Res.*, *88*: 760–769, 1997.
- Lawrence, R. A., Izbicka, E., De Jager, R. L., Tohgo, A., Clark, G. M., Weitman, S. D., Rowinsky, E. K., and Von Hoff, D. D. Comparison of DX-8951f and topotecan effects on tumor colony formation from freshly explanted adult and pediatric human tumor cells. *Anticancer Drugs*, *10*: 655–661, 1999.
- Joto, N., Ishii, M., Minami, M., Kuga, H., Mitsui, I., and Tohgo, A. DX-8951f, a water-soluble camptothecin analog, exhibits potent antitumor activity against a human lung cancer cell line and its SN-38-resistant variant. *Int. J. Cancer*, *72*: 680–686, 1997.
- Ishii, M., Iwahana, M., Mitsui, I., Minami, M., Imagawa, S., Tohgo, A., and Ejima, A. Growth inhibitory effect of a new camptothecin analog, DX-8951f, on various drug-resistant sublines including BCRP-mediated camptothecin derivative-resistant variants derived from the human lung cancer cell line PC-6. *Anticancer Drugs*, *11*: 353–362, 2000.
- Kumazawa, E., Jimbo, T., Ochi, Y., and Tohgo, A. Potent and broad antitumor effects of DX-8951f, a water-soluble camptothecin derivative, against various human tumors xenografted in nude mice. *Cancer Chemother. Pharmacol.*, *42*: 210–220, 1998.
- Bouvet, M., Yang, M., Nardin, S., Wang, X., Jiang, P., Baranov, E., Moossa, A. R., and Hoffman, R. M. Chronologically-specific metastatic targeting of human pancreatic tumors in orthotopic models. *Clin. Exp. Metastasis*, *18*: 213–218, 2000.
- Bouvet, M., Wang, J., Nardin, S. R., Nassirpour, R., Yang, M., Baranov, E., Jiang, P., Moossa, A. R., and Hoffman, R. M. Real-time optical imaging of primary tumor growth and multiple metastatic events in a pancreatic cancer orthotopic model. *Cancer Res.*, *62*: 1534–1540, 2002.
- Yang, M., Jiang, P., Sun, F. X., Hasegawa, S., Baranov, E., Chishima, T., Shimada, H., Moossa, A. R., and Hoffman, R. M. A fluorescent orthotopic bone metastasis model of human prostate cancer. *Cancer Res.*, *59*: 781–786, 1999.
- Fu, X., Guadagni, F., and Hoffman, R. M. A metastatic nude-mouse model of human pancreatic cancer constructed orthotopically with histologically intact patient specimens. *Proc. Natl. Acad. Sci. USA*, *89*: 5645–5649, 1992.
- Yang, M., Baranov, E., Jiang, P., Sun, F. X., Li, X. M., Li, L., Hasegawa, S., Bouvet, M., Al-Tuwaijri, M., Chishima, T., Shimada, H., Moossa, A. R., Penman, S., and Hoffman, R. M. Whole-body optical imaging of green fluorescent protein-expressing tumors and metastases. *Proc. Natl. Acad. Sci. USA*, *97*: 1206–1211, 2000.
- JD'Adamo, D., Hammond, L., Donehower, R., Sharma, S., Aird, S., Kelsen, D. P., Ochoa, L., Rowinsky, E., De Jager, R., and O'Reilly, E. M. Final results of a Phase II study of Exatecan Mesylate (DX-8951f, DX) in advanced pancreatic cancer. *Proc. Am. Soc. Clin. Oncol.*, *20*: 134a, 2001.
- O'Reilly, E. M., Lenzi, R., Mani, M., Schwartz, G. K., Sharma, S., Kelsen, D., Levin, A., Danna, M., Hazelwood, B., and De Jager, R. A Phase I study of DX-8951f (Exatecan Mesylate, DX) and gemcitabine (Gem) in advanced solid tumor malignancies. *Proc. Am. Soc. Clin. Oncol.*, *21*: 99a, 2002.
- Hoffman, R. M. Orthotopic metastatic mouse models for anticancer drug discovery and evaluation: a bridge to the clinic. *Investig. New Drugs*, *17*: 343–359, 1999.
- Hoffman, R. M. Green fluorescent protein imaging of tumour growth, metastasis, and angiogenesis in mouse models. *Lancet Oncol.*, *3*: 546–556, 2002.